Self-Assembling Molecular Trees Containing Octa- p -phenylene: From Nanocrystals to Nanocapsules

ARTICLE *in* JOURNAL OF THE AMERICAN CHEMICAL SOCIETY · JUNE 2004

Impact Factor: 12.11 · DOI: 10.1021/ja048856h · Source: PubMed

8 AUTHORS, INCLUDING:

Soojin Park
Ulsan National Institute of Science and Tech…
149 PUBLICATIONS **4,078** CITATIONS

SEE PROFILE

Taihyun Chang
Pohang University of Science and Technology
248 PUBLICATIONS **5,807** CITATIONS

SEE PROFILE

J|A|C|S
ARTICLES
Published on Web 04/30/2004

Self-Assembling Molecular Trees Containing Octa-*p*-phenylene: From Nanocrystals to Nanocapsules

Yong-Sik Yoo,[†] Jin-Ho Choi,[†] Ji-Ho Song,[†] Nam-Keun Oh,[‡] Wang-Cheol Zin,[‡] Soojin Park,[§] Taihyun Chang,[§] and Myongsoo Lee*,[†]

Contribution from the Center for Supramolecular Nano-Assembly and Department of Chemistry, Yonsei University, Shinchon 134, Seoul 120-749, Korea, and the Departments of Materials Science and Engineering and Chemistry, Pohang University of Science and Technology, Pohang 790-784, Korea

Received March 1, 2004; E-mail: mslee@yonsei.ac.kr

Abstract: Tree-shaped molecules consisting of octa-*p*-phenylene as a stem segment and oligoether dendrons as a flexible head were synthesized and characterized. The molecular tree based on a small flexible head self-assembles into a lamellar structure, whereas the molecule based on a larger headgroup self-assembles into a discrete heptameric bundle that organizes into a 3-D primitive orthorhombic supercrystals, as confirmed by X-ray scatterings and transmission electron microscopic (TEM) observations. Optical studies revealed that the absorption and emission maxima and absorption edge of the 3-D structure shift to higher energy compared to those of the lamellar structure. The molecules in dilute solution (THF/water = 1:10 v/v) were observed to self-assemble into capsule-like hollow aggregates, as confirmed by dynamic and static light scatterings, scanning electron microscopy (SEM), and TEM investigations. These results demonstrate that tree-shaped molecules are capable of packing into organized discrete nanocrystals with parallel arrangement as well as hollow nanocapsules with radial arrangement, depending on the presence of selective solvents for flexible headgroup.

Introduction

An emerging field of chemistry involves the design and synthesis of self-assembling molecules that organize into regular organic nanostructures.[1] Self-assembling molecules based on conjugated rod building blocks promise the opportunity to explore desired functions and properties as a result of aggregation into well-defined supramolecular architectures.[2] Thus, diverse molecular structures are being created as a means of manipulating aggregation structure which has dramatic effects on the physical properties of materials. Incorporation of a conjugated rod into a block molecular architecture leads to a novel class of self-assembling molecules, where the anisotropic orientation of the rod segments and repulsion between the covalently connected segments lead to self-organization into unique aggregation structures.[3] The aggregation architectures and the properties can be tuned by careful selection of the type and relative length of the respective blocks.

Previous publications from our laboratory reported synthesis and structural analysis of rod−coil block systems that self-assemble into lamellar, cylindrical, and discrete nanostructures depending on the relative volume fraction of the rod segments.[4] In addition, we have demonstrated that rod−coil systems with an elongated rod block self-assemble into discrete bundles or perforated layers that organize into 3-D tetragonal or 3-D hexagonal superlattices, respectively.[5] The shape and size of the aggregation structure have also been reported to have a strong influence on the photophysical properties of conjugated molecular materials.[6] Thus, manipulation of aggregation structure in conjugated systems is of paramount importance in achieving desirable properties in supramolecular materials.

[†] Yonsei University.
[‡] Department of Materials Science and Engineering, Pohang University of Science and Technology.
[§] Department of Chemistry, Pohang University of Science and Technology.

(1) (a) Lehn, J. M. *Supramolecular Chemistry, Concepts and Perspectives*; VCH: Weinheim, Germany, 1995. (b) Muthukumar, M.; Ober, C. K.; Thomas, E. L. *Science* **1997**, *277*, 1225−1232. (c) Stupp, S. I.; LeBonheur, V.; Walker, K.; Li, L. S.; Huggins, K. E.; Kesser, M.; Amstutz, A. *Science* **1997**, *276*, 384−389. (d) Lee, M.; Cho, B.-K.; Zin, W.-C. *Chem. Rev.* **2001**, *101*, 3869−3892.
(2) (a) Segura, J. L.; Martin, N. *J. Mater. Chem.* **2000**, *10*, 2403−2435. (b) Kraft, A.; Grimsdale, A. C.; Holmes, A. B. *Angew. Chem., Int. Ed.* **1998**, *37*, 402−428. (c) Bunz, U. H. F. *Acc. Chem. Res.* **2001**, *34*, 998−1010. (d) Breen, C. A.; Deng, T.; Breiner, T.; Thomas, E. L.; Swager, T. *J. Am. Chem. Soc.* **2003**, *125*, 9942−9943. (e) Berresheim, A. J.; Müller, M.; Müllen, K. *Chem. Rev.* **1999**, *99*, 9. 1747−1786.
(3) (a) Leclere, P.; Calderone, A.; Marsitzky, D.; Francke, V.; Geertz, Y.; Müllen, K.; Bredas, J. L.; Lazzaroni, R. *Adv. Mater.* **2000**, *12*, 1042−1046. (b) Hempenius, M. A.; Langeveld-Voss, B. M. W.; van Haar, J. A. E. H.; Janssen, R. A. J.; Sheiko, S. S.; Spatz, J. P.; Möller, M.; Meijer, E. W. *J. Am. Chem. Soc.* **1998**, *120*, 2798−2804. (c) Wang, H.; Wang, H. H.; Urban, V. S.; Littrel, K. C.; Thiyagarajan, P.; Yu, L. *J. Am. Chem. Soc.* **2000**, *122*, 6855−6861. (d) Jenekhe, S. A.; Chen, X. L. *Science* **1999**, *283*, 372−375. (e) Jenekhe, S. A.; Chen, X. L. *Science* **1998**, *279*, 1903−1907. (f) Kilbinger, A. F. M.; Schenning, A. P. H. J.; Goldoni, F.; Feast, W. J.; Meijer, E. W. *J. Am. Chem. Soc.* **2000**, *122*, 1820−1821.
(4) (a) Lee, M.; Cho, B.-K.; Kim, H.; Yoon, J.-Y.; Zin, W.-C. *J. Am. Chem. Soc.* **1998**, *120*, 9168−9179. (b) Lee, M.; Lee, D.-W.; Cho, B.-K.; Yoon, J.-Y.; Zin, W.-C. *J. Am. Chem. Soc.* **1998**, *120*, 13258−13259.
(5) (a) Lee, M.; Cho, B.-K.; Jang, Y.-G.; Zin, W.-C. *J. Am. Chem. Soc.* **2000**, *122*, 7449−7455. (b) Lee, M.; Cho, B.-K.; Ihn, K. J.; Lee, W.-K.; Oh, N.-K.; Zin, W.-C. *J. Am. Chem. Soc.* **2001**, *123*, 4647−4648.
(6) Lee, M.; Jeong, Y.-S.; Cho, B.-K.; Oh, N.-K.; Zin, W.-C. *Chem.−Eur. J.* **2002**, *8*, 876−883.

 10.1021/ja048856h CCC: $27.50

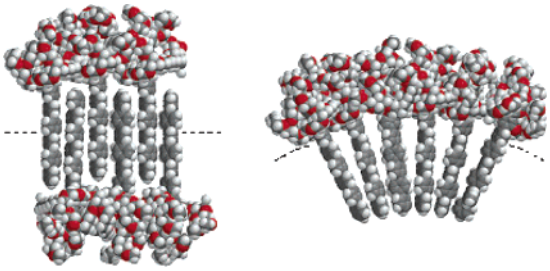

Figure 1. Schematic representation of the molecular arrangement of molecular trees. (a) Interdigitated parallel arrangement of molecules and (b) orientationally ordered radial arrangement of molecules.

A strategy to manipulate the aggregation structure assembled from a conjugated rod building block may be accessible by connecting hydrophilic, flexible dendritic branches to its one side, leading to a tree-shaped molecule. The molecular tree based on small branches may self-assemble into a monolayer lamellar structure in which the rod segments are fully interdigitated, similar to simple rod−coil molecules. As the volume fraction of the flexible part of the molecule increases, greater steric repulsion between adjacent flexible parts could possibly cause an increment in the interfacial area to relieve repulsive forces, giving rise to the formation of a discrete nanostructure maintaining parallel arrangement of rod segments (Figure 1a).[1d,7,8] Furthermore, tree-shaped molecules can also be considered as an amphiphilic molecule because they consist of hydrophilic dendritic chains as a head and a hydrophobic rod as a stem. When such molecules with an amphiphilic character are dissolved in hydrophilic solvents, the molecules may self-assemble into aggregates with interfacial curvature surrounded by the hydrophilic flexible chains due to hydrophobic effect. In contrast to bulk nanocrystals with parallel arrangement of rod segments, rod segments in a selective solvent would be packed with orientationally ordered radial arrangement to maximize the contact of the hydrophilic chains with water, giving rise to a unique supramolecular structure with interfacial curvature (Figure 1b). Therefore, amphiphilic tree-shaped molecules can provide the unique possibility to change the nanostructure from discrete nanocrystals to spherical aggregates by introduction of selective solvent to flexible chains.

In this article, we describe the synthesis of tree-shaped molecules consisting of octa-*p*-phenylene as a stem segment and oligo(ethylene oxide) dendrons as flexible branches and the self-assembling behavior in the bulk and dilute THF/water (1:10 v/v) solution characterized by optical polarized microscopy, differential scanning calorimetry (DSC), powder X-ray diffraction, transmission electron microscopy (TEM), scanning electron microscopy (SEM), and light scattering measurements. The molecular tree based on a small hydrophilic head self-assembles into a lamellar structure, whereas the molecule containing a large head crystallizes into a discrete nanostructure that organizes into a 3-D primitive orthorhombic supercrystal. In dilute solution, however, the molecules self-assemble into a hollow nanocapsule, as confirmed by a combination of light scattering, TEM, and SEM measurements.

Experimental Section

4-Trimethylsilyl-biphenyl-4′-boronic acid, 4-diphenyl boronic acid, 1,4-dibromo-2,5-dimethoxybenzene (**3a**), and dendritic oligoether coils ($\mathbf{R_1}$ and $\mathbf{R_2}$) were prepared according to the similar procedures described previously.[9,10] For synthetic detail, see the Supporting Information. ^{1}H NMR and ^{13}C NMR spectra were recorded from $CDCl_3$ solutions on a Bruker AM 250 or 500 spectrometer. The purity of the products was checked by thin-layer chromatography (TLC; Merck, silica gel 60). A Perkin-Elmer DSC-7 differential scanning calorimeter equipped with 1020 thermal analysis controller was used to determine the thermal transitions, which were reported as the maxima and minima of their endothermic or exothermic peaks. In all cases, the heating and cooling rates were 10 °C/min. A Nikon Optiphot 2-pol optical polarized microscopy (magnification: 100 ×) equipped with a Mettler FP 82 hot-stage and a Mettler FP 90 central processor was used to observe the thermal transitions and to analyze the anisotropic texture. Microanalyses were performed with a Perkin-Elmer 240 elemental analyzer. X-ray scattering measurements were performed in transmission mode with synchrotron radiation at the 3C2 X-ray beam line at Pohang Accelerator Laboratory, Korea. Molecular weight distribution ($\bar{M}_w/\bar{M}_n$) was determined by gel permeation chromatography (GPC) with a Waters R401 instrument equipped with Stragel HR 3, 4, and 4E columns, M7725i manual injector, column heating chamber, and 2010 Millennium data station. MALDI-TOF mass was performed on a Perseptive Biosystems Voyager-DE STR using a 2,5-dihydroxy benzoic acid matrix. The molecular density (ρ) measurements were performed in aqueous sodium chloride solution at 25 °C. Optical absorption spectra were obtained from a Shimadzu 1601 UV spectrophotometer. The steady-state fluorescence spectra were obtained from a Hitachi F-4500 fluorescence spectrophotometer. The SEM was recorded on a Hitachi S-4200 at an acceleration voltage of 18 kV. A drop of the solution (1×10^{-5} g/mL in THF/water 1:10 v/v) was put on Al foil and dried under reduced pressure. The sample was then coated with gold in the ion coater for 30 s. The TEM was performed at 120 kV using JEOL JEM 2010. The sample was embedded in epoxy resin and microtomed at −170 °C using a cyro-ultramicrotome without staining. Light scattering experiments were performed using a light scattering goniometer (BI200-SM, Brookhaven Instruments) equipped with a digital autocorrelator (BI-9000 AT, Brookhaven Instruments) and an Ar ion laser (Model 95, Lexel Laser Inc.). The incident light was vertically polarized at $\lambda = 488$ nm, and the typical laser power was 75 mW. All the measurements were carried out at the temperature of 25.0 ± 0.1 °C. Dynamic (DLS) and static light scattering (SLS) experiments were performed over a scattering angular range of 30° to 120° at the sample concentrations range of 5.0×10^{-6} to 1.0×10^{-5} g/mL. The hydrodynamic radius of the self-assembly was determined from the analysis of the DLS autocorrelation functions by the cumulants and the CONTIN methods using the software provided by the manufacturer. The radius of gyration and the molecular weight of the self-assembly of the molecular tree were obtained by Zimm plot of the SLS intensity. The specific refractive index increments, d*n*/d*c*, in water/THF mixture was determined as 0.201 mL/g by differential refractometry.

Results and Discussion

Synthesis. The synthesis of treelike molecules consisting of octa-*p*-phenylene as a stem segment and oligoether dendrons as flexible branches is outlined in Scheme 1 and start with the preparation of 1,4-dibromo-2,5-dimethoxybenzene and oligoether dendrons according to the procedures described previously.[9,10] Trimethylsilyl-substituted biphenyl derivative **4a** was prepared from the Suzuki coupling reaction of **3b** in the presence

(7) Semenov, A. N. *Mol. Cryst. Liq. Cryst.* **1991**, *209*, 191.
(8) Williams, D. R. M.; Fredrickson, G. H. *Macromolecules* **1992**, *25*, 3561−3568.
(9) Vahlenkamp, T.; Wegner, G. *Macromol. Chem. Phys.* **1994**, *195*, 1933−1952.
(10) Jayaraman, M.; Frechet, J. M. J. *J. Am. Chem. Soc.* **1998**, *120*, 12996−12997.

Scheme 1. Synthesis of Molecular Tree **1** and **2**

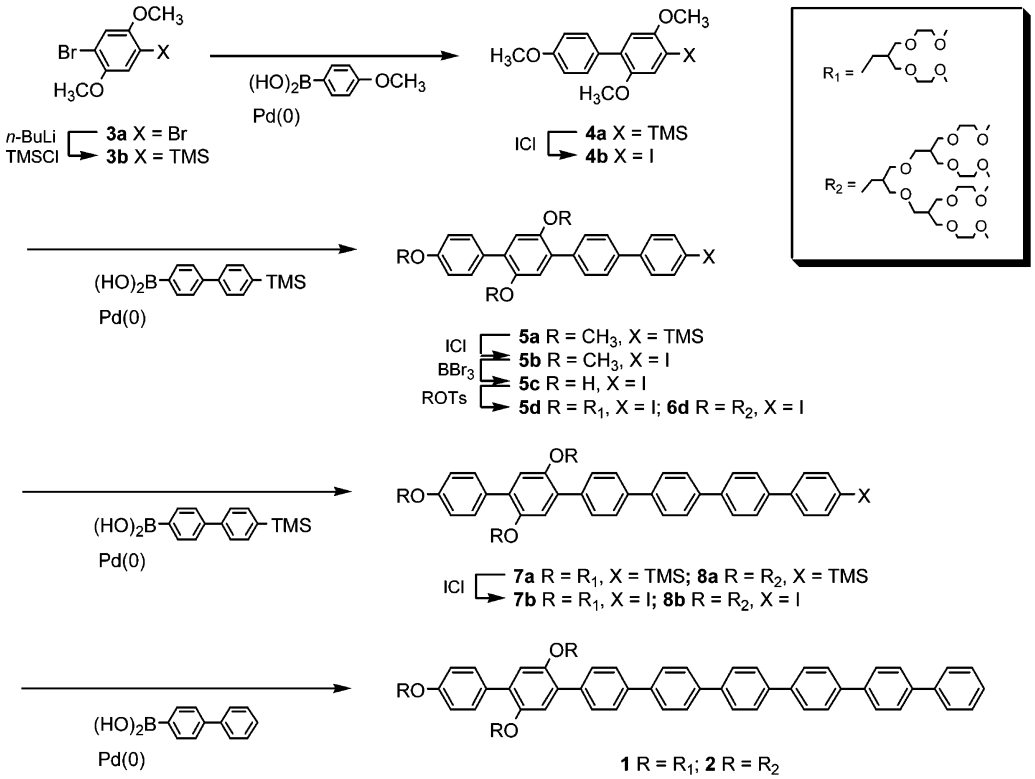

of Pd(0) catalysis.[11] For the next Suzuki coupling reaction, the trimethylsilyl group of **4a** was substituted to aryl iodide, which is the most active in Suzuki-type aromatic couplings, and then subsequent aromatic coupling reaction produced **5a**. After iodination of **5a** with ICl, the methoxy groups in the molecule were deprotected, and then the subsequent etherification with tosylated oligoether dendrons yielded **5d** and **6d**, showing sufficient solubility for further couplings of rigid conjugated building blocks in the reaction medium. The final tree-shaped molecules were synthesized by following the same sequence of reactions, i.e., by Suzuki coupling reaction of **5d** and **6d** with 4-bromobiphenyl-4′-boronic acid, subsequent iodination with ICl, and finally, reaction with 4-biphenyl boronic acid. All of the resulting tree-shaped molecules were purified by silica gel column chromatography and subsequent reprecipitation of diethyl ether solution to *n*-hexane as described in the Experimental Section. The resulting tree-shaped molecules were characterized by NMR spectroscopy, elemental analysis, GPC, and MALDI-TOF mass spectroscopy. As confirmed by ^{1}H NMR spectroscopy, the ratio of the aromatic protons of the rod block to the ethylene oxide protons is consistent with the ratio calculated according to the number of dendritic units and octa-*p*-phenylene. As shown in Figure 2, the MALDI-TOF mass spectra of the molecular trees exhibit three signals that can be assigned as the molecular ions, together with the Na^+ and K^+ labeled molecular ions. The mass corresponding to a representative peak in the spectrum is matched with the calculated molecular weight of each of the molecular trees.

Solid State Structure. The self-assembling behavior of the tree-shaped molecules in the bulk was investigated by means of DSC, thermal optical polarized microscopy, TEM, and X-ray scatterings. The molecules show an ordered structure, and the

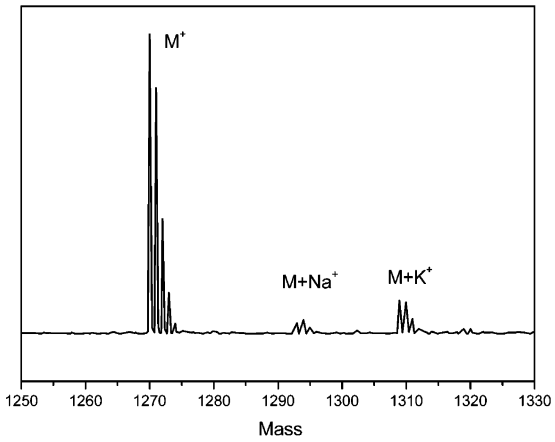

Figure 2. MALDI-TOF mass spectrum of **1**.

transition temperatures and the corresponding enthalpy changes are determined from DSC scans. The molecular trees appear to be opaque waxy solid that melts into isotropic liquid at 135.3 °C and 76.6 °C for **1** and **2**, respectively (Figure 3a). Between cross polarizers, these waxy solids showed strong birefringence. Although no discernible texture could be identified from **1**, **2** showed a characteristic texture associated with supramolecular ordering. On cooling from the optically isotropic phase of **2**, rectangular areas growing in four directions can be observed with a final development of mosaic texture, characteristics of a tetragonal structure exhibited by rod−coil systems (Figure 3b).[5,6]

To corroborate the solid-state structure of the molecular trees, small- and wide-angle X-ray scattering experiments were performed. The small-angle X-ray diffraction pattern of **1** based on a small head displays sharp reflections that correspond to equidistant *q*-spacings and thus index to a lamellar lattice. The layer spacing of 4.2 nm is very close to the estimated molecular

(11) Miyaura, N.; Suzuki, A. *Chem. Rev.* **1995**, *95*, 2457−2483.

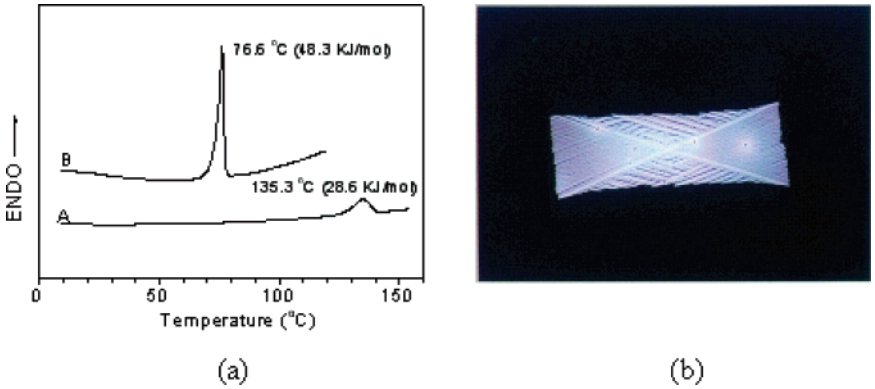

Figure 3. (a) DSC curves recorded during the first heating scan of (A) **1** and (B) **2**. (b) Representative optical polarized micrograph (100×) of the texture exhibited by **2** at the transition from the isotropic state at 76 °C.

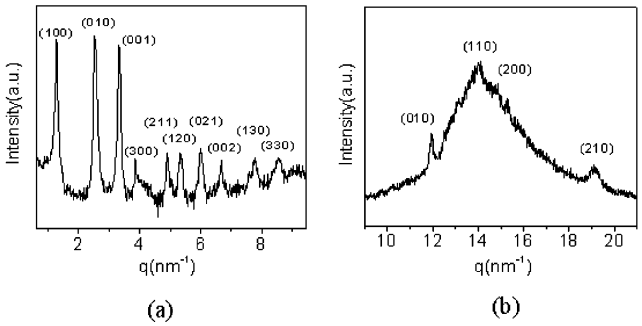

Figure 4. (a) Small-angle X-ray diffraction pattern of **2** measured at 25 °C. (b) Wide-angle X-ray diffraction pattern of **2** measured at 25 °C.

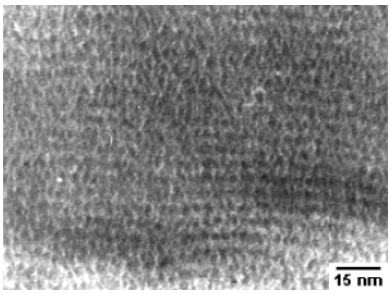

Figure 5. Transmission electron micrograph of **2** without staining.

length, indicating that the rods are packed into a fully interdigitated monolayer lamellar structure (see Supporting Information). The wide-angle X-ray diffraction pattern shows a strong peak which is due to crystal packing of the rod segments. The small-angle X-ray diffraction pattern of **2** based on a large flexible head shows three strong reflections together with a number of low intensity reflections at higher angles (Figure 4a), indicative of the existence of a highly ordered nanoscopic structure with three distinct lattice parameters. These reflections indeed can be indexed as a 3-D primitive orthorhombic structure with lattice parameters $a = 2.5$ nm, $b = 1.9$ nm, and $c = 4.9$ nm.[12] The wide-angle X-ray diffraction pattern shows several sharp reflections corresponding to a rectangular lattice with unit cell dimensions of $x = 8.5$ Å and $y = 5.2$ Å, indicating that the rod building blocks are arranged in a herringbone fashion within the domains (Figure 4b).

When microtomed films of **2** without the use of stains were characterized by TEM, dark domains in a lighter matrix could be observed as shown in Figure 5. The dark regions are believed to consist of crystalline rod blocks, similar to other rod−coil systems reported previously.[13] The image reveals that the average diameter of the aggregates is roughly 2 nm, which is comparable to the lattice parameters determined from small-angle X-ray diffraction pattern.

On the basis of the optical and transmission electron microscopic observations and X-ray diffraction results, tree-shaped molecule **2** can be considered to self-assemble into discrete bundles encapsulated by ether chains that organize into a 3-D primitive orthorhombic supercrystal. Calculation based on the lattice parameters of the 3-D unit cell and measured densities indicates that the number of molecules in each bundle is about seven.[14] The tendency of the rod building blocks to be arranged into anisotropic crystalline order along their axes is likely to generate nonspherical aggregates, which are responsible for the formation of the 3-D orthorhombic superlattice. Furthermore, this orthorhombic nature with three characteristic dimensions, together with a rectangular crystalline lattice, suggests that the aggregation of seven molecules in each aggregate generates the heptameric bundle with cross sections that are more rectangular than circular in shape (Figure 6).

Both steric forces and crystallization are believed to play an important role in the formation of discrete heptameric bundle. Treelike molecules based on a small flexible head would be packed into a continuous 2-D sheetlike structure as in the case of **1**. Increasing the volume fraction of the head causes the steric forces among head parts to be greater. This increase in steric repulsion could drive the sheetlike domain to break up into discrete nanostructures that allow more space for the flexible chains to adopt a less strained conformation.[7,8,15] Accordingly, **2** based on a large flexible head is likely to self-organize into a discrete 3-D structure with prolate shape.

Absorption and Emission Studies. The effects of supramolecular structure on the bulk state optical properties were investigated by using the UV/vis absorption and fluorescence spectroscopies. Figure 7 shows the absorption and fluorescence spectra of the treelike molecules and of the CH_2Cl_2 solution of

(12) Kitamura, M.; Nakano, K. *Cryst. Growth Des.* **2003**, *3*, 25−34.
(13) Tew, G. N.; Pralle, M. U.; Stupp, S. I. *J. Am. Chem. Soc.* **1999**, *121*, 9852−9866.

(14) From the three characteristic lattice parameters (a, b, and c) determined from SAXS and the molecular density (r), the average number of molecule per bundle (n) can be calculated according to eq 1, where M is the molecular mass and N_A is Avogadro's number:

$$n = \frac{abc}{\{M\}/\{N_A\rho\}}$$

(15) Müller, M.; Schick, M. *Macromolecules* **1996**, *29*, 8900−8903.

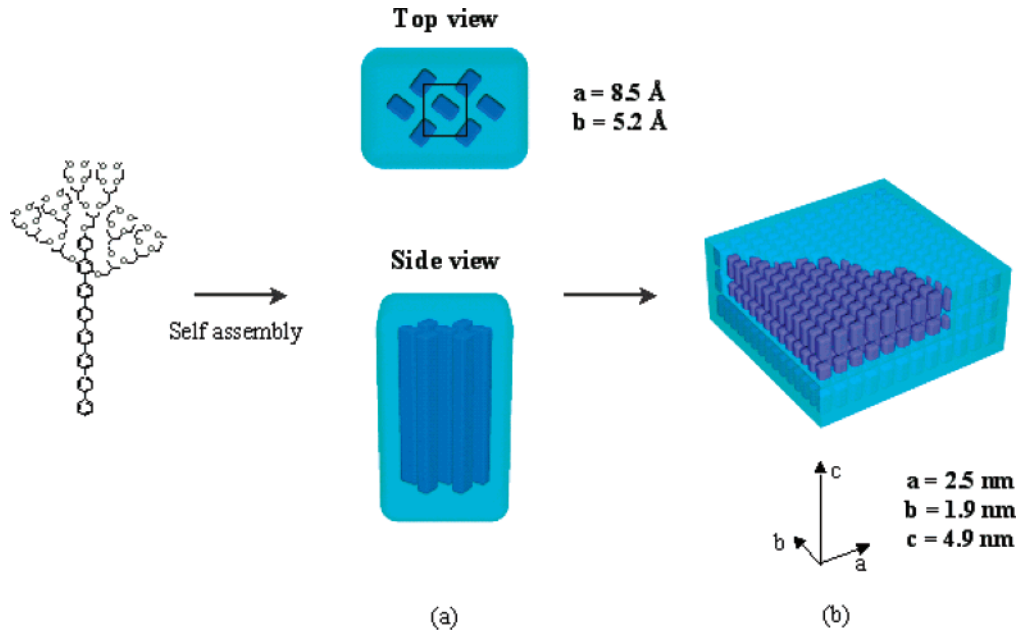

Figure 6. Schematic representation of (a) the self-assembly of **2** into a discrete bundle with the herringbone packing of the octa-*p*-phenylene rods and (b) the subsequent crystallization into a primitive orthorhombic superlattice.

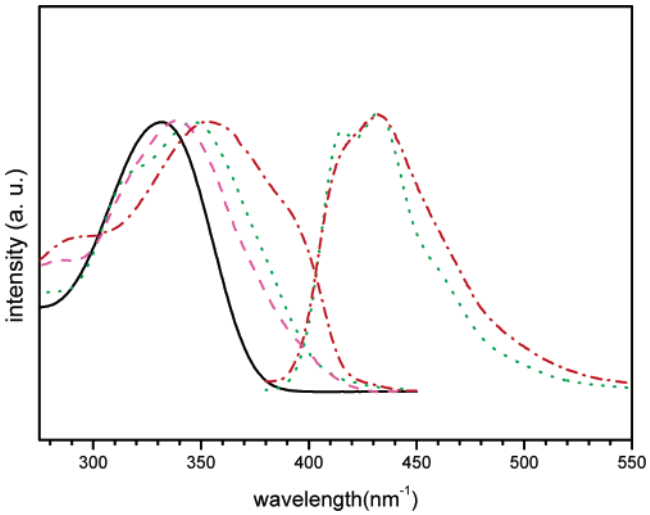

Figure 7. Absorption and emission spectra of **1** and **2**. (Solid line) absorption (left) of **2** in CH_2Cl_2 solution. (Dashed line) absorption of solid thin film of **2** prepared from the THF/water (1:10 v/v) solution with concentration of 1×10^{-5} g/mol. (Dotted line) absorption (left) and emission (right) of solid film of **2**. (Dash−dotted line) absorption (left) and emission (right) of solid film of **1**.

2 for comparison. Both the absorption and emission spectra of thin solid films of the molecules appear to be red-shifted with respect to those of the corresponding solutions and thus demonstrate existence of intermolecular interactions or increase in the planarization of conjugated rod segments due to crystal packing. In the bulk state, both the absorption maximum and absorption edge of **2** shift to higher energy relative to those of **1**. Furthermore, the intensity of the emission band centered at about 415 nm of **2** increases at the expense of the intensities corresponding to 460 and 500 nm, in comparison with the emission profile of **1**.

These results could be attributed to nanosize effect of the optically active discrete nanostructure. As evidenced by TEM and small-angle X-ray scatterings, the supramolecular structure of **2** consists of three-dimensionally confined rod domains encapsulated by flexible segments, in contrast to that of **1**, where the rods are packed into sheetlike continuous domains. Therefore, this 3-D confinement of optically active domains in dimensions less than 10 nm is presumably responsible for this interesting optical behavior. The absorption and emission maxima and absorption edge in semiconducting nanoparticles have also been observed to shift to higher energy with decreasing particle size in the range less than 10 nm.[16,17] This trend may also arise from the slightly different intermolecular interactions between adjacent conjugated rods that occur with variation in the headgroup size of the molecular tree.[18−20] However, the size effect and intermolecular interactions seem to be cooperative, and their contribution could be equally important in the optical properties of the supramolecular materials.

Self-Assembly in Aqueous Solution. Amphiphilic block molecules, when dissolved in a selective solvent for one of the blocks, can self-assemble into a variety of aggregate structures, including vesicular structures.[21] The molecular trees can be considered as a new class of amphiphiles because they consist of a hydrophobic rod and a hydrophilic flexible head. Aggregation behavior of the molecular trees was subsequently studied in water by dissolving a molecular tree solution in THF (1.1×10^{-4} g/mL) into ultrapure water, which gave a final THF/water ratio of 1:10 v/v. After the solutions were allowed to equilibrate over 24 h, the aggregation structure was investigated by using both DLS and SLS, TEM, and field emission scanning electron microscopy (FE-SEM). Dynamic light scattering experiments

(16) Henglein, A. *Chem. Rev.* **1989**, *89*, 1861−1873.
(17) Murray, C. B.; Norris, D. J.; Bawendi, M. G. *J. Am. Chem. Soc.* **1993**, *115*, 8706−8715.
(18) Cacialli, F.; Wilson, J. S.; Michels, J. J.; Daniel, C.; Silva, C.; Friend, R. H.; Severin, N.; Samori, P.; Rabe, J. P.; O'Connell, M. J.; Tayor, P. N.; Anderson, H. L. *Nat. Mater.* **2002**, *1*, 160−164.
(19) Fu, H.-B.; Yao, J.-N. *J. Am. Chem. Soc.* **2001**, *123*, 1434−1439.
(20) Lee, J.-K.; Koh, W.-K.; Chae, W.-S.; Kim, Y.-R. *Chem. Commun.* **2002**, 138−139.
(21) (a) Alexandridis, P.; Lindman, B. *Amphiphilic Block Copolymer, Self-Assembly and Applications*; Elservier: New York, 2000. (b) Antonietti, M.; Förster, S. *Adv. Mater.* **2003**, *15*, 1323−1333. (c) Discher, D. E.; Eisenberg, A. *Science* **2002**, *297*, 967−973. (d) Förster, S.; Plantenberg, T. *Angew. Chem., Int. Ed.* **2002**, *41*, 688−714.

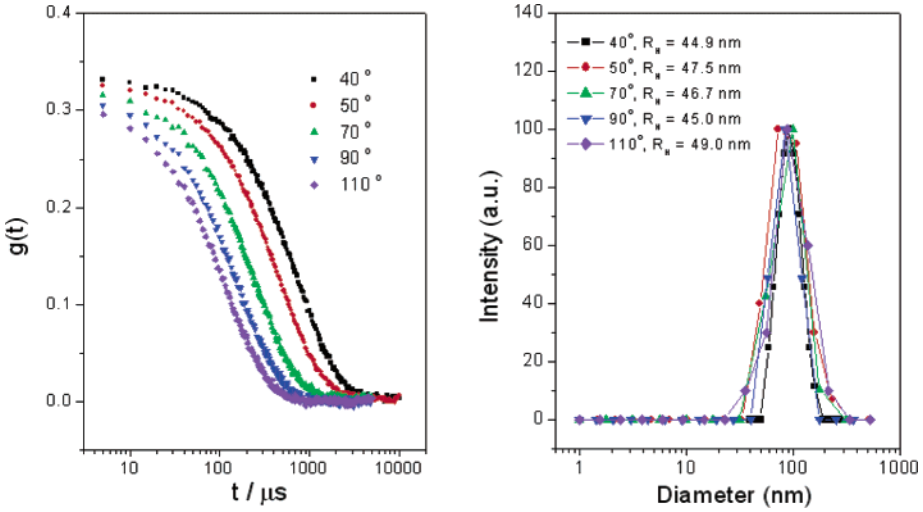

Figure 8. Autocorrelation function (left) and hydrodynamic radius distribution (right) of **2** in THF/water (1:10 v/v) solution with concentration of 1×10^{-5} g/mL.

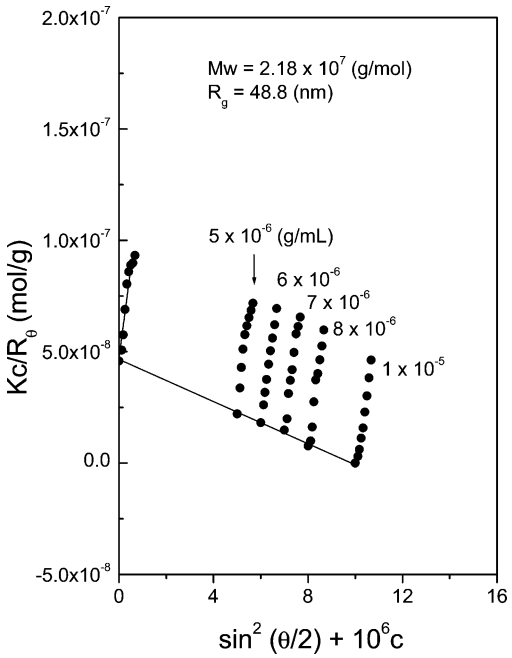

Figure 9. Zimm plot of **2** in THF/water (1:10 v/v) solution, obtained at 25 °C over a concentration range of 1×10^{-5} to 5×10^{-6} g/mL.

were performed with the solutions of **1** and **2** with concentration of 1×10^{-5} g/mL over a scattering angular range of 30° to 120° and a concentration range of 5×10^{-6} g/mL to 1×10^{-5} g/mL at 25 °C. The aggregate size was estimated using the CONTIN analysis for evaluation of the autocorrelation function.[22−24] In both cases, the analysis of the autocorrelation functions showed a monomodal size distribution, thus confirming the formation of only one family of aggregate sizes (Figure 8), indicating well-equilibrated structures without unimers and impurities. The average hydrodynamic radii (R_H) of the corresponding aggregates were observed to be approximately 100 nm for **1** and 46 nm for **2**, indicating that the molecular tree with a larger flexible headgroup assembles into a smaller size of aggregate.

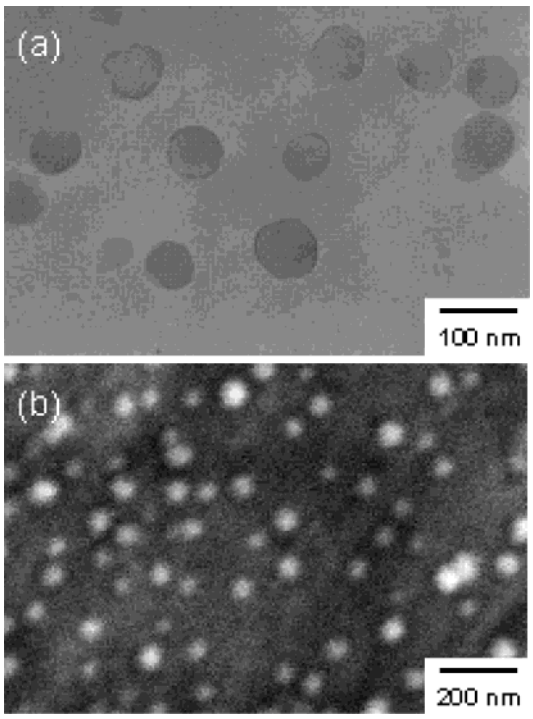

Figure 10. (a) TEM and (b) SEM images of capsules of **2**.

To get more information about the size and the molecular weight of the aggregates, SLS measurements were performed with **2** under the same conditions. Figure 9 shows an example of the Zimm plot of the results of **2** solutions. From the Zimm plots, the weight-averaged molecular weight (M_w) was found to be 2.18×10^7 g/mol. In addition, the radius of gyration (R_g) was found to be 48.8 nm. Thus, the radius of gyration of **2** is nearly identical to the hydrodynamic radius determined from DLS, suggesting the existence of hollow spheres.[24,25] The measured diameter exceeds the extended molecular lengths (approximately 4 nm) by a factor of about 20, also strongly suggesting that these aggregates are rather capsule-like entities than simple micelles. TEM studies on this sample revealed that there is the obvious contrast between the periphery and center

(22) Koppel, D. E. *J. Chem. Phys.* **1972**, *57*, 4814−4820.
(23) Provencher, S. W. *Makromol. Chem.* **1979**, *180*, 201−209.
(24) Zhou, S.; Burger, C.; Chu, B.; Sawamura, M.; Nagahama, N.; Toganoh, M.; Hackler, U. E.; Isobe, H.; Nakamura, E. *Science* **2001**, *291*, 1944−1947.
(25) Chu, B. *Laser Light Scattering*, 2nd ed.; Academic Press: New York, 1991.

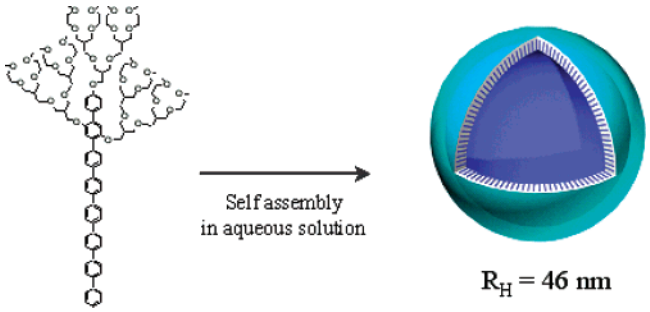

Figure 11. Schematic representation of formation of the nanocapsule in solution state.

in the sphere, characteristic of the projection images of hollow spheres (Figure 10a).[21c] The formation of nanocapsule of **2** was also confirmed by FE-SEM experiments. As shown in Figure 10b, the SEM micrograph shows spherical aggregates that are approximately 80 nm in diameter and are thus consistent with the results obtained from light scattering experiments. On the basis of results described above, a schematic representation can be illustrated as shown in Figure 11.

Conclusions

New treelike amphiphilic molecules consisting of octa-*p*-phenylene as a stem and oligo(ethylene oxide) dendrons as branches were synthesized, and their self-assembling behavior was investigated in the solid and dilute THF/water solution (1:10 v/v). The molecular tree based on a small flexible head was observed to self-assemble into a monolayer lamellar structure, whereas the molecule based on a larger headgroup self-assembled into a heptameric bundle that self-organizes into a 3-D primitive orthorhombic supercrystal. Spectroscopic studies of the molecular trees demonstrated the supramolecular structure has a strong influence on the photophysical properties of the optically active materials. In dilute solutions, the molecules were observed to self-assemble into capsule-like aggregates in which the rod building blocks are likely to be assembled with radial arrangement.

Compared to other self-assembling systems, including block copolymers,[21,26,27−30] surfactant molecules,[31] and liquid crystals,[32] the molecular tree possesses the unique feature that the rigid building block is capable of packing into organized discrete nanocrystals with parallel arrangement as well as hollow nanocapsules with radial arrangement in one system, depending on the presence of selective solvents. These results demonstrate that rational design of a self-assembling molecule based on a conjugated rod building block allows stable nanostructures to be produced. These nanostructures potentially have a number of applications, including the encapsulation and controlled release of active species and nanoreactors.

Acknowledgment. This work was supported by National Creative Research Initiative Program of the Korean Ministry of Science and Technology. We thank Pohang Accelerator Laboratory, Korea, for allowing us to use the Synchrotron Radiation Source. T.C. acknowledges a financial support from KOSEF (Center for Intergrated Molecular Systems).

Supporting Information Available: Experimental details, ^{13}C NMR and MALDI-TOF of **2**, and SAXS of **1** (PDF). This material is available free of charge via the Internet at http://pubs.acs.org.

JA048856H

(26) (a) Vriezema, D. M.; Hoogbum, J.; Velonia, K.; Takazawa, K.; Christianen, P. C. M.; Maan, J. C.; Rowan, A. E.; Nolte, R. J. M. *Angew. Chem., Int. Ed.* **2003**, *42*, 772−776. (b) Holder, S. J.; Hiorns, R. C.; Sommerdijk, N. A. J. M.; Williams, S. J.; Jones, R. G.; Nolte, R. J. M. *Chem. Commun.* **1998**, 1445−1446.
(27) Kukula, H.; Schlaad, H.; Antonietti, M.; Förster, S. *J. Am. Chem. Soc.* **2002**, *124*, 1658−1663.
(28) Checot, F.; Lecommandoux, S.; Gnanou, Y.; Klok, H.-A. *Angew. Chem., Int. Ed.* **2002**, *41*, 1339−1343.
(29) Discher, B. M.; Won, Y.-Y.; Ege, D. S.; Lee, J. C.-M.; Bates, F. S.; Discher, D. E.; Hammer, D. A. *Science* **1999**, *284*, 1143−1146.
(30) Nardin, C.; Hirt, T.; Leukel, J.; Meier, W. *Langmuir* **2000**, *16*, 1035−1041.
(31) Hamley, I. W. *Introduction to Soft Matter*; Wiley-VCH: Weinheim, Germany, 2000; Chapter 4.
(32) (a) Collings, P. J.; Hird, M. *Introduction to Liquid Crystals, Chemistry and Physics*; Taylor & Francis: London, 1997. (b) Tschierske, C. *J. Mater. Chem.* **2001**, *11*, 2647−2671.